J Surfact Deterg (2018) **21:** 139–153
DOI 10.1002/jsde.12015

ORIGINAL ARTICLE

Nuclear Magnetic Resonance Investigation of the Effect of pH on Micelle Formation by the Amino Acid-Based Surfactant Undecyl L-Phenylalaninate

Gabriel A. Rothbauer[1] · Elisabeth A. Rutter[1] · Chelsea Reuter-Seng[1] · Simon Vera[2] · Eugene J. Billiot[2] · Yayin Fang[3] · Fereshteh H. Billiot[2] · Kevin F. Morris[1]

Received: 27 July 2017 / Revised: 10 October 2017 / Accepted: 8 November 2017

Abstract Micelle formation by the anionic amino acid-based surfactant undecyl L-phenylalaninate (und-Phe) was investigated as a function of pH in solutions containing either Na^+, L-arginine, L-lysine, or L-ornithine counterions. In each mixture, the surfactant's critical micelle concentration (CMC) was the lowest at low pH and increased as solutions became more basic. Below pH 9, surfactant solutions containing L-arginine and L-lysine had lower CMC than the corresponding solutions with Na^+ counterions. Nuclear magnetic resonance (NMR) diffusometry and dynamic light scattering studies revealed that und-Phe micelles with Na^+ counterions had hydrodynamic radii of approximately 15 Å throughout the investigated pH range. Furthermore, L-arginine, L-lysine, and L-ornithine were found to bind most strongly to the micelles below pH 9 when the counterions were cationic. Above pH 9, the counterions became zwitterionic and dissociated from the micelle surface. In und-Phe/L-arginine solution, counterion dissociation was accompanied by a decrease in the hydrodynamic radius of the micelle. However, in experiments with L-lysine and L-ornithine, micelle radii remained the same at low pH when counterions were bound and at high pH when they were not. This result suggested that L-arginine is attached perpendicular to the micelle surface through its guanidinium functional group with the remainder of the molecule extending into solution. Contrastingly, L-lysine and L-ornithine likely bind parallel to the micelle surface with their two amine functional groups interacting with different surfactant monomers. This model was consistent with the results from two-dimensional ROESY (rotating frame Overhauser enhancement spectroscopy) NMR experiments. Two-dimensional NMR also showed that in und-Phe micelles, the aromatic rings on the phenylalanine headgroups were rotated toward the hydrocarbon core of micelle.

Keywords Amino acid surfactant · Micelle · Counterion · NMR

J Surfact Deterg (2018) **21:** 139–153.

Abbreviations

CE	capillary electrophoresis
CMC	critical micelle concentration
DLS	dynamic light scattering
HPLC	high-performance liquid chromatography
NMR	nuclear magnetic resonance
NOESY	nuclear Overhauser effect spectroscopy
ROESY	rotating frame Overhauser enhancement spectroscopy
TMS	tetramethylsilane
und-Leu	undecylenyl L-leucine
und-Phe	L-undecyl phenylalaninate

Introduction

Amino acid-based surfactants are biodegradable, biocompatible, have low toxicity, and can be produced using

✉ Kevin F. Morris
kmorris@carthage.edu

[1] Department of Chemistry, Carthage College, 2001 Alford Park Drive, Kenosha, WI 53140, USA

[2] Department of Physical and Environmental Sciences, Texas A&M University-Corpus Christi, 6300 Ocean Drive, Corpus Christi, TX 78412, USA

[3] Department of Biochemistry and Molecular Biology, Howard University College of Medicine, Howard University, 520 W Street NW, Washington, DC, 20059, USA

Published online: 14 February 2018
J Surfact Deterg (2018) **21:** 139–153

renewable materials (Bordes & Holmberg, 2015; Brito & Silva, 2011; Chandra & Tyagi, 2013; Clapes & Infante, 2002; Infante, Perez, Pinazo, & Vinardell, 2004). Because of their emulsifying and antimicrobial properties, they are also used in the pharmaceutical, food, and cosmetic industries (Chandra & Tyagi, 2013). Amino acid-based surfactants contain a polar amino acid or a peptide headgroup bound to one or more hydrophobic hydrocarbon chains. In aqueous solution, the hydrocarbon chains have low affinity for the solvent, while the polar headgroups experience favorable interactions with the aqueous phase. Therefore, above a critical concentration or critical micelle concentration (CMC), amino acid-based surfactants aggregate into micelles with small spherical or long, rod-like shapes (Bordes & Holmberg, 2015; Brito & Silva, 2011; Chandra & Tyagi, 2013; Clapes & Infante, 2002; Infante et al., 2004). The amino acid or peptide headgroups align with the micelle–water interface, while the nonpolar hydrophobic tails interact with one another in the micelle core, which can also solubilize nonpolar materials present in solution (Bordes & Holmberg, 2015; Brito & Silva, 2011; Chandra & Tyagi, 2013; Clapes & Infante, 2002; Infante et al., 2004).

In this study, micelle formation by a phenylalanine-containing amino acid-based surfactant was investigated. The aggregation behavior of similar molecules has been reported in the literature. For example, surfactants containing lauryl esters of L-phenylalanine bound to aliphatic chains of varying lengths have been studied by Vijay et al. (2010a, 2010b) using nuclear magnetic resonance (NMR), electron spin resonance, and fluorescence spectroscopy. Solutions containing these surfactants were found to form large, 50–200 nm micelles in which the surfactants' phenylalanine aromatic ring was rotated toward the micelle's hydrocarbon core. Micelle radii were also found to scale linearly with the solution's specific optical rotation values (Covington & Polavarapu, 2016; Vijay, Baskar, Mandal, & Polavarapu, 2013). The synthesis and surface-active properties of sodium *N*-acylphenylalanine surfactants prepared from natural oils (Sreenu, Prasad, Sujitha, & Kumar, 2015) and anionic phenylalanine-glycerol ether surfactants have also been reported (Varka, Coutouli-Argyropoulou, Infante, & Pegiadou, 2004). Finally, cationic phenylalanine-based surfactants have been found to interact with model membranes and to have antimicrobial activity (Joondan, Jhaumeer-Laulloo, & Caumul, 2014).

In this study, the anionic surfactant undecyl L-phenylalaninate (und-Phe) was investigated. The molecule's structure is shown in Fig. 1a. The atom labels in Fig. 1 are used in the two-dimensional NMR analyses described below. Micelles formed by amino acid-based surfactants similar to und-Phe but containing valine or leucine headgroups have been used as chiral selectors in capillary electrophoresis (CE) (Ramos et al., 2017; Sciba, 2016). This study investigated how the pH of the solution affected the CMC and radii of und-Phe micelles along with the micelles' ability to bind to Na^+, L-arginine, L-lysine, and L-ornithine counterions. In CE, separations with L-undecyl leucinate, L-arginine, and L-lysine counterions were found to affect the chiral resolution of binaphthyl compounds (Ramos et al., 2017). The chemical structures of L-arginine, L-lysine, and L-ornithine are shown in Figs. 1b–d, respectively. Figure 1 shows the cationic forms of the three amino acids present in solution below pH 9. In this form, the amino acid counterions are expected to bind through an electrostatic attraction to the surface of the anionic und-Phe micelles.

CMC measurements were made with NMR spectroscopy by monitoring the change in the chemical shifts of the und-Phe aromatic and NH proton resonances as a function of solution concentration. Micelle radii and the fraction of surfactant monomers and amino acid counterions bound to the micelles were investigated with pulsed gradient NMR diffusion experiments. NMR-derived micelle radii in solutions containing und-Phe and $NaHCO_3$ were also compared to radii from dynamic light scattering (DLS) experiments. Finally, the structures of intermolecular complexes formed by und-Phe and both L-arginine and L-lysine counterions were studied with two-dimensional NMR. Results were compared to those from previously reported work with L-undecyl leucinate (und-Leu) and to the behavior of other phenylalanine-based surfactants.

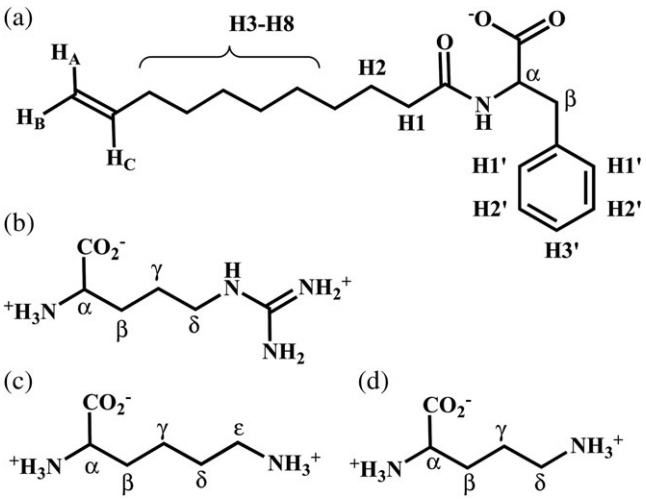

Fig. 1 Structures of (**a**) L-undecyl phenylalaninate, (**b**) L-arginine, (**c**) L-lysine, and (**d**) L-ornithine. Atom labels are used to assign the two-dimensional NMR spectra. Cationic forms of the amino acid counterions found in solution below pH 9.0 are shown

Experimental Details

Solution Preparation

All reagents were purchased from Sigma Aldrich (Milwaukee, WI, USA). Solutions containing the surfactant and equimolar concentrations of $NaHCO_3$ (99.5%), L-lysine (≥98%), L-arginine (≥98%), or L-ornithine (≥98%) were prepared gravimetrically. The solvent used in the NMR studies was 90% deionized water and 10% deuterium oxide (99.9% atom). Solution pH was adjusted by adding either $NaOH_{(s)}$ (97%) or concentrated $DCl_{(aq)}$ to the surfactant solutions. This method was used in order to minimally affect the total volume of solution. A three-point calibration of the pH meter was performed before each measurement. Solutions used in the NMR diffusion experiments were also spiked with a small volume of tetramethylsilane (≥99.9%) (TMS), which was added directly into each NMR tube. Solutions were then vortexed, passed through a 0.2-μm syringe filter, and allowed to equilibrate at 25.0°C before NMR measurements were made.

Surfactant Synthesis

Undecyl L-phenylalaninate was prepared by reacting the *N*-hydroxysuccinimide ester of undecylenic acid with L-phenylalanine (Lipidot, Rappoport, & Wolman, 1967). NMR spectroscopy was used to confirm the purity of the surfactants. An NMR spectrum of a mixture containing 50.0 mM und-Phe and 50.0 mM $NaHCO_3$ is included in the Supporting Information.

Critical Micelle Concentration

In the CMC measurements, stock solutions containing 50 mM und-Phe and 50 mM of either $NaHCO_3$, L-arginine, or L-lysine were prepared in 90% H_2O, 10% D_2O. Dilutions were then made to produce solutions with und-Phe concentrations ranging from 1 to 25 mM. The concentrations of either $NaHCO_3$, L-arginine, or L-lysine were held constant at 50 mM. Proton NMR spectra were then collected for each sample using the Watergate water suppression method to reduce the H_2O signal (Piotto, Saudek, & Skienar, 1992). The chemical shifts of the NH proton at 7.6 ppm and the two aromatic resonances at 7.3 and 7.2 ppm were then recorded. Representative NMR spectra showing changes in the und-Phe chemical shifts with increasing surfactant concentration are shown in Fig. 2a.

The chemical shift (ppm) of the aromatic and NH resonances were then plotted against the inverse of solution concentration as shown in Fig. 2b. The data were fit to two straight lines: one below the CMC and one above the CMC. The point at which the two lines intersected was then determined and taken as the inverse of the CMC (MacInnis, Palepu, & Marangoro, 1999; Shimizu, Pires, & El Seoud, 2003). Three replicate CMC measurements were made for each mixture.

DLS Measurements

Dynamic light scattering (DLS) measurements were performed using a Malvern Nano Series Zetasizer at a scattering angle of 90°. The DLS instrument contained a He–Ne laser with a wavelength and power of 532 nm and 50 mW, respectively. All solvents used for DLS measurements were passed through a 0.20 μm filter and the pH of the surfactant solutions were adjusted as described above. After preparation, surfactant solutions were filtered again before DLS measurements were made.

NMR Diffusion Experiments

The radii of the und-Phe micelles and the binding of cationic counterions to the anionic micelle surface were investigated with NMR diffusion experiments. These experiments are described in detail by Lewis et al. (2016). To summarize, a series of NMR spectra were collected with increasing magnetic field gradient strength, G, using the bipolar pulse pair longitudinal encode–decode pulse sequence (Wu, Chen, & Johnson, 1995). Typical G values ranged from 5 to 50 G cm^{-1}. The intensity of NMR resonances in these experiments decayed exponentially with a rate proportional to the quantity, $(\gamma \cdot G \cdot \delta)^2 \cdot (\Delta - \delta/3 - \tau/3)$, where γ is the magnetogyric ratio, δ is the duration of the magnetic field gradient pulses, τ is the short delay between the bipolar gradient pulses, and Δ is the diffusion time (Lewis et al., 2016; Wu et al., 1995). The Δ, δ, and τ values used in this study were 250, 4.0, and 0.20 ms, respectively. A plot of the natural log of peak intensity *versus* $(\gamma \cdot G \cdot \delta)^2 \cdot (\Delta - \delta/3 - \tau/3)$ produced a straight line with a slope equal to $-D$ (Lewis et al., 2016; Wu et al., 1995). Figure 3 shows a representative diffusion plot for each component in a sample containing 50 mM und-Phe, 50 mM L-arginine, and TMS at pH 8.0.

Rotating Frame Overhauser Enhancement Spectroscopy NMR

Phase-sensitive rotating frame Overhauser enhancement spectroscopy (ROESY) spectra were acquired by collecting 400 transients for each of 256 increments and 2048 data points in the F1 and F2 dimensions, respectively. Linear prediction was used to extend the data set in the F1 dimension by 200 points and zero filling was carried out to generate a 2048 × 1024 point data set. A $\pi/2$-shifted sine-bell-squared apodization function was applied

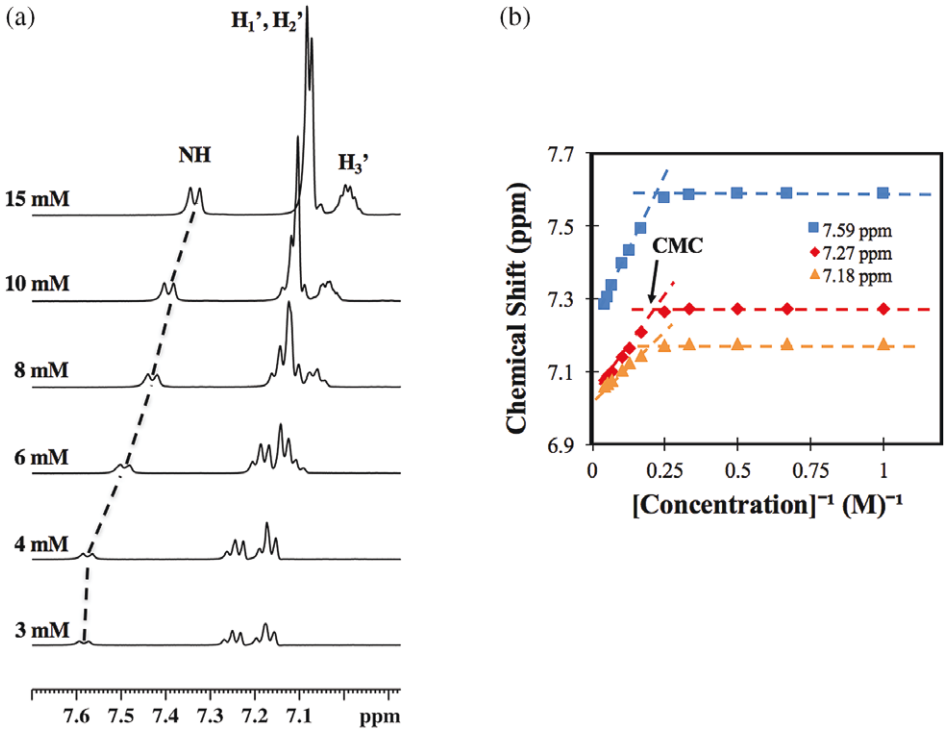

Fig. 2 (**a**) Proton NMR spectra as a function of surfactant concentration for und-Phe/L-arginine mixtures at pH 9.0. (**b**) Representative plot of chemical shift *versus* inverse concentration used to calculate the CMC

in F1 and F2 and then the data set was Fourier transformed and phased in both dimensions. The ROESY spin lock time was 200 ms.

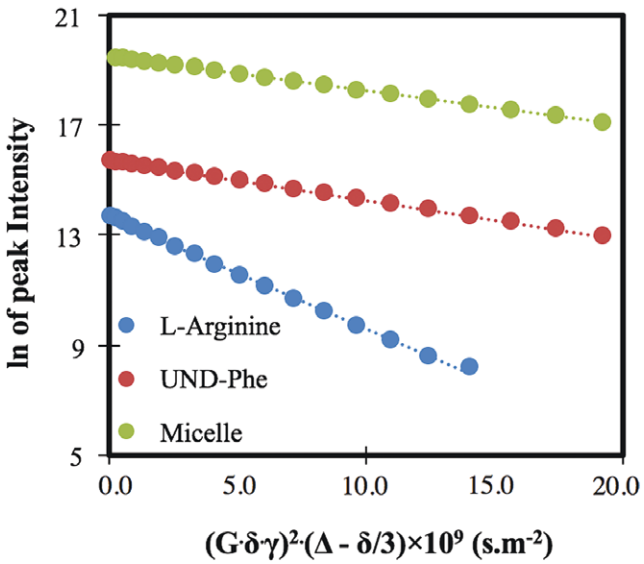

Fig. 3 Plot of the natural log of peak intensity *versus* $(\gamma \cdot G \cdot \delta)^2 \cdot (\Delta - \delta/3 - \tau/2)$ for a mixture containing 50 mM und-Phe and 50 mM L-arginine at pH 8. The slope of each line is $-D$. The mixture was spiked with a small amount of tetramethyl silane (TMS). The plot labeled micelle represents the decay of the TMS peak intensity

Viscosity Measurements

For each und-Phe:counterion mixture, viscosity measurements were made with a capillary Oswald viscometer at pH 7.0, 8.0, 9.0, 10, and 11.0 using the method reported previously (Lewis et al., 2016). All measurements were made at 25.0°C. The pH-averaged viscosity for each mixture was then calculated and used in the micelle radii calculations described below. An analogous method was used in a previous NMR study of the amino acid-based surfactant und-Leu (Lewis et al., 2016).

Results and Discussion

CMC Measurements

Table 1 reports the CMC of und-Phe as a function of pH for solutions containing Na^+ counterions. These data show that the CMC of und-Phe was 5.8 mM at pH 7.5. The CMC increased slightly to 8.6 mM at pH 11.5. A similar trend was seen in a study of the surfactant und-Leu, which also had a lower CMC below pH 9 and a slightly higher CMC at more basic pH (Lewis et al., 2016). The CMC *versus* pH trend in Table 1 may result in part from some fraction of the surfactant molecules having a protonated carboxylate group at lower pH values. When an und-Phe

Table 1 D_{obs} (und-Phe), $D_{micelle}$, und-Phe f_b values, NMR-derived micelle hydrodynamic radii (R_h), CMC, and DLS-derived micelle hydrodynamic radii *versus* pH for und-Phe solutions containing Na^+ counterions

pH	$D_{obs} \times 10^{10}$ und-Phe (m^2 s^{-1})	$D_{micelle} \times 10^{10}$ (m^2 s^{-1})	f_b und-Phe	R_h (Å) NMR	CMC (mM)	R_h (Å) DLS
7.5	1.88 ± 0.09	1.71 ± 0.07	0.958 ± 0.017	14.1 ± 0.6	5.8 ± 0.1	13.6 ± 0.5
8.0	1.82 ± 0.01	1.57 ± 0.08	0.943 ± 0.006	15.3 ± 0.8	6.0 ± 0.1	16.4 ± 0.2
8.5	1.80 ± 0.01	1.64 ± 0.01	0.962 ± 0.006	14.7 ± 0.1	7.0 ± 0.6	16.6 ± 0.8
9.0	1.91 ± 0.11	1.74 ± 0.14	0.960 ± 0.019	13.8 ± 0.1	7.0 ± 0.5	14.1 ± 0.5
9.5	1.69 ± 0.01	1.55 ± 0.01	0.967 ± 0.006	15.5 ± 0.1	7.8 ± 0.1	13.2 ± 0.7
10.0	1.97 ± 0.01	1.62 ± 0.02	0.920 ± 0.006	14.9 ± 0.2	8.1 ± 0.3	14.1 ± 0.4
10.5	1.64 ± 0.01	1.54 ± 0.01	0.977 ± 0.007	15.6 ± 0.1	7.9 ± 0.3	14.9 ± 0.7
11.0	1.65 ± 0.01	1.54 ± 0.01	0.974 ± 0.007	15.7 ± 0.1	8.4 ± 0.3	16.7 ± 0.5
11.5	1.73 ± 0.09	1.61 ± 0.09	0.973 ± 0.017	14.9 ± 0.8	8.6 ± 0.5	15.8 ± 0.4

At each pH, the und-Phe concentration was 50.0 mM and the temperature was 25.0°C.

molecule's carboxylate is protonated, the surfactant is neutral and, therefore, more nonpolar than the corresponding deprotonated, anionic surfactant molecule. As a result, the neutral surfactant is more likely to aggregate into micelles, thus lowering the CMC.

It is also interesting to note the difference between the und-Leu/Na^+ and und-Phe/Na^+ CMC values. Even though both solutions experienced the same overall trend—lower CMC at low pH, higher CMC at high pH—the CMC of the und-Leu surfactant reported by Lewis et al. (2016)) was approximately 20 mM over the investigated pH range, while the CMC of und-Phe ranged from 5.8 to 8.6 mM. This result is expected because the aromatic amino acid side chain in und-Phe is more nonpolar than the isobutyl side chain of und-Leu. Therefore, the nonpolar, aromatic side chain of und-Phe makes the surfactant overall more hydrophobic and causes the surfactant to aggregate into micelles at a lower concentration than und-Leu.

CMC values for the und-Phe surfactant in solutions containing 50 mM L-arginine are shown in Table 2. The structure of L-arginine is shown in Fig. 1b. Below pH 9.0, both the primary and side-chain amine functional groups of L-arginine are protonated. Therefore, in this pH range, the L-arginine molecules are cationic and bind to the surface of the anionic und-Phe micelles. Table 2 shows that the L-arginine-containing und-Phe solutions have a CMC of 3.4 mM below pH 9.0. The CMC in the arginine-containing solutions begins to increase at pH 9.5 and becomes approximately 9.8 mM at high pH. Koyama (2005) investigated micelle formation by octanoic, decanoic, lauric, and myristic fatty acids in the presence of L-arginine counterions. The Koyama study found an inverse relationship between the degree of counterion binding to the micelle and the surfactant's CMC. For example, when the mole fraction of bound L-arginine molecules, $f_{b,Arg}$, was high, the surfactants' CMC values were low and *vice versa* (Koyama, 2005). The same trend is evident in the data from Table 2, which also reports the mole fraction of micelle-bound L-arginine molecules, $f_{b,Arg}$. These values were measured with NMR diffusion experiments and are discussed in more detail below. The Table 2 results show that at low pH, $f_{b,Arg}$ values are the highest and the CMC values are

Table 2 D_{obs} (und-Phe), $D_{micelle}$, $D_{arginine}$, und-Phe f_b values, L-arginine f_b values, micelle hydrodynamic radii (R_h), and CMC *versus* pH for und-Phe solutions containing L-arginine counterions

pH	$D_{obs} \times 10^{10}$ und-Phe (m^2 s^{-1})	$D_{micelle} \times 10^{10}$ (m^2 s^{-1})	$D_{Arg} \times 10^{10}$ (m^2 s^{-1})	f_b und-Phe	f_b L-arginine	R_h (Å)	CMC (mM)
7.5	1.49 ± 0.01	1.39 ± 0.01	4.99 ± 0.02	0.979 ± 0.009	0.464 ± 0.004	16.2 ± 0.1	3.4 ± 0.1
8.0	1.36 ± 0.01	1.19 ± 0.01	4.05 ± 0.01	0.964 ± 0.007	0.587 ± 0.003	19.0 ± 0.1	3.4 ± 0.2
8.5	1.44 ± 0.01	1.24 ± 0.01	4.01 ± 0.11	0.958 ± 0.007	0.596 ± 0.014	18.2 ± 0.1	3.4 ± 0.2
9.0	1.37 ± 0.01	1.26 ± 0.01	4.55 ± 0.01	0.976 ± 0.007	0.587 ± 0.003	17.9 ± 0.2	4.1 ± 0.1
9.5	1.40 ± 0.01	1.26 ± 0.01	4.82 ± 0.02	0.972 ± 0.008	0.480 ± 0.003	17.8 ± 0.1	4.9 ± 0.1
10.0	1.68 ± 0.01	1.47 ± 0.01	5.88 ± 0.04	0.952 ± 0.007	0.335 ± 0.056	15.4 ± 0.1	5.7 ± 0.1
10.5	1.71 ± 0.01	1.56 ± 0.01	6.94 ± 0.02	0.967 ± 0.007	0.177 ± 0.002	14.4 ± 0.1	8.2 ± 0.1
11.0	1.77 ± 0.01	1.65 ± 0.01	7.08 ± 0.11	0.973 ± 0.008	0.158 ± 0.017	13.6 ± 0.1	9.7 ± 0.1
11.5	1.86 ± 0.05	1.71 ± 0.06	7.39 ± 0.14	0.965 ± 0.013	0.112 ± 0.023	13.2 ± 0.1	9.8 ± 0.1

At each pH, the und-Phe concentration was 50.0 mM and the temperature was 25.0 °C.

3.4 mM. As the pH is increased, the $f_{b,Arg}$ values decrease and there is a corresponding increase in the surfactant's CMC. The results shown in Table 2 are, therefore, consistent with the observations made by Koyama (2005).

Table 3 reports und-Phe CMC values for solutions containing 50 mM L-lysine. Like L-arginine, L-lysine is cationic below pH 9.0. The CMC values for the und-Phe solutions containing L-lysine are similar to the Table 2 results for L-arginine. Table 3 shows that the CMC of the und-Phe/L-lysine micelles is approximately 4.0 mM below pH 9.0. At pH 9.5, the CMC begins to increase and becomes approximately 8.0 mM above pH 10. It is also interesting to note that below pH 9.0 where the CMC was the lowest, the corresponding $f_{b,Lys}$ value was highest and *vice versa.* Therefore, the results obtained for the L-lysine-containing solutions were also consistent with those of the Koyama study, which also showed an inverse relationship between counterion fraction bound values and surfactants' CMC values (Koyama, 2005).

Finally, one notable difference between the Na^+ and the L-arginine/L-lysine CMC results is that below pH 9.5, the und-Phe CMC values are lower for the L-arginine/L-lysine containing solutions and higher for the solutions containing Na^+ counterions. These results suggest that in their cationic state, L-arginine and L-lysine molecules facilitate the formation of und-Phe micelles. Below pH 9.0, both the L-arginine and L-lysine primary and side chain amine functional groups are protonated. As a result, und-Phe may, as shown in Fig. 4, form species below the CMC with one L-arginine or L-lysine molecule bound to two und-Phe surfactants. This behavior is not possible in the presence of Na^+, which has a single +1 charge. If L-arginine/L-lysine and und-Phe molecules interact below the CMC as shown in Fig. 4, this effect may help bring together und-Phe surfactant molecules, allowing them to form micelles at a lower concentration. The Koyama study (2005) of fatty acid aggregation also found that fatty acid solutions containing bulkier counterions like L-arginine had lower CMC values than solutions with smaller counterions like Na^+. Here at low pH, smaller CMC values were also measured for und-Phe solutions containing the bulkier L-arginine and L-lysine counterions. On the other hand, while the size of the counterion may indeed play a role, other factors such as the ability of the counterions to bridge multiple surfactant molecules as shown in Fig. 4 are likely important as well.

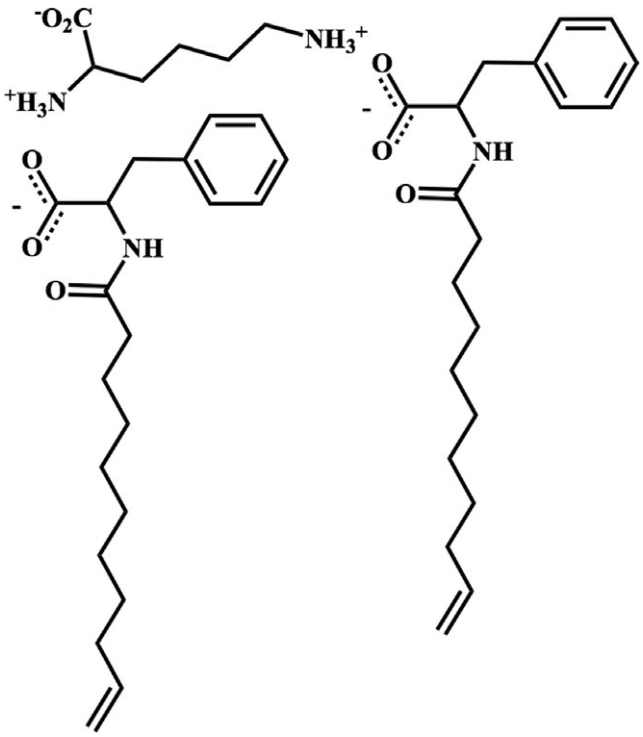

Fig. 4 L-Lysine binding simultaneously to two und-Phe surfactant molecules. The cationic form of the amino acid found in solution below pH 9.0 is shown

Table 3 D_{obs} (und-Phe), $D_{micelle}$, D_{lysine}, und-Phe f_b values, L-lysine f_b values, micelle hydrodynamic radii (R_h), and CMC *versus* pH for und-Phe solutions containing L-lysine counterions

pH	$D_{obs} \times 10^{10}$ und-Phe ($m^2\ s^{-1}$)	$D_{micelle} \times 10^{10}$ ($m^2\ s^{-1}$)	$D_{lys} \times 10^{10}$ ($m^2\ s^{-1}$)	f_b und-Phe	f_b L-lysine	R_h (Å)	CMC (mM)
7.5	1.69 ± 0.02	1.46 ± 0.02	5.43 ± 0.04	0.949 ± 0.021	0.404 ± 0.008	15.2 ± 0.2	3.9 ± 0.1
8.0	1.68 ± 0.01	1.49 ± 0.02	5.62 ± 0.03	0.959 ± 0.018	0.376 ± 0.007	14.8 ± 0.2	4.0 ± 0.1
8.5	1.65 ± 0.01	1.44 ± 0.01	5.52 ± 0.02	0.955 ± 0.017	0.389 ± 0.006	15.4 ± 0.1	4.5 ± 0.4
9.0	1.72 ± 0.10	1.49 ± 0.09	6.29 ± 0.02	0.947 ± 0.033	0.275 ± 0.007	14.9 ± 0.9	5.4 ± 0.3
9.5	1.65 ± 0.01	1.43 ± 0.01	6.71 ± 0.05	0.952 ± 0.017	0.210 ± 0.009	15.5 ± 0.1	6.1 ± 0.1
10.0	1.68 ± 0.01	1.46 ± 0.01	7.41 ± 0.04	0.953 ± 0.017	0.106 ± 0.007	15.1 ± 0.1	6.2 ± 0.1
10.5	1.74 ± 0.02	1.47 ± 0.01	8.12 ± 0.03	0.941 ± 0.017	0.052 ± 0.011	15.1 ± 0.1	8.1 ± 0.1
11.0	1.82 ± 0.01	1.60 ± 0.01	7.47 ± 0.01	0.951 ± 0.017	0.100 ± 0.005	13.8 ± 0.1	7.8 ± 0.1
11.5	1.67 ± 0.01	1.39 ± 0.01	7.76 ± 0.02	0.941 ± 0.017	0.053 ± 0.005	15.9 ± 0.1	7.6 ± 0.1

At each pH, the und-Phe concentration was 50.0 mM and the temperature was 25.0°C.

Micelle Radii and Counterion Binding

NMR translational self-diffusion is a well-established method for quantifying micelle radii and the degree of counterion binding to surfactant micelles. (Gnezdilov, Zuev, Zueva, Potarikina, & Us'yarov, 2011; Lewis et al., 2016; Stilbs, 1987; Stilbs & Lindman, 1981). The later can also be investigated by monitoring changes in counterion chemical shift as a function of concentration (Bijma & Engberts, 1997; Singh, Singh, & Kang, 2016; Xing, Lin, Lu, & Xian, 2008). In the diffusion measurements reported here, the translational diffusion coefficient, D, was measured for each component in the und-Phe surfactant mixtures. These components included the und-Phe micelles and either L-arginine, L-lysine, or L-ornithine counterions. The solutions investigated were also spiked with a small amount of TMS. The TMS molecules solubilized inside the und-Phe micelles, allowing for the determination of the und-Phe micelle diffusion coefficient, D_{micelle}, through an analysis of the decaying TMS signal (Stilbs, 1987). This value was substituted into the Stokes–Einstein equation to calculate the hydrodynamic radii, R_{h}, of the und-Phe micelles (Stilbs, 1987). The viscosity values used in the radii calculations were 0.907, 0.967, 0.986, and 0.905 cp for und-Phe solutions containing Na^+, L-arginine, L-lysine, and L-homoarginine, respectively. Viscosities were measured at 25.0°C with a capillary Oswald viscometer using the method reported previously (Lewis et al., 2016).

The TMS probe method used to measure D_{micelle} has been used in other NMR studies of micelle diffusion (Annunziata, Costantino, D'Errico, Paduano, & Vitagliano, 1999; D'Errico, Ornella, Paduano, & Vitagliano, 2001; Morris, Gao, & Wong, 2004; Phani Kumar, Priyadharsini, Prameela, & Mandal, 2011; Vitiello, Ciccarelli, Ortona, & D'Errico, 2009). It also allows the micelle diffusion coefficient to be established in a single experiment in which both und-Phe and counterion concentrations are 50.0 mM. An alternative method for determining D_{micelle} is to measure the und-Phe diffusion coefficient ($D_{\text{obs,und-Phe}}$) as a function of surfactant concentration (C). A plot is then prepared of $D_{\text{obs,und-Phe}}$ *versus* C^{-1}. The micelle diffusion coefficient is the y-intercept of this plot (Begotka, Hunsader, Oparaeche, Vincent, & Morris, 2006; Fournial et al., 2007; Orfi, Lin, & Larive, 1998). To assess the reliability of the TMS probe method used here, radii for micelles containing und-Phe and Na^+ counterions were also measured with DLS. The DLS results are given in Table 1 and discussed in more detail below. Overall, the NMR and DLS radii were found to be in good agreement, suggesting that the TMS probe method provides reasonable estimates of und-Phe D_{micelle} values.

The und-Phe surfactant molecules undergo fast exchange between the micelle and free solution. Therefore, as shown in Eq. 1, the diffusion coefficient reported by the und-Phe resonances, $D_{\text{obs,und-Phe}}$, is the weighted average of the micelle bound, D_{micelle}, and free solution, $D_{\text{und-Phe, free}}$, values (Gnezdilov et al., 2011; Stilbs, 1987; Stilbs & Lindman, 1981).

$$D_{\text{obs,und-Phe}} = f_{\text{b,und-Phe}} \times D_{\text{micelle}} + (1 - f_{\text{b,und-Phe}}) D_{\text{und-Phe,free}} \quad (1)$$

$D_{\text{und-Phe, free}}$ was found to be $6.04(\pm 0.05) \times 10^{-10}$ m^2 s^{-1} and $f_{\text{b,und-Phe}}$ is the mole fraction of und-Phe molecules bound to the micelles (Stilbs, 1987).

In an analogous fashion, cationic L-arginine, L-lysine, or L-ornithine counterions bound to the und-Phe micelles also undergo fast exchange between bound and free solution states (Gnezdilov et al., 2011; Stilbs, 1987; Stilbs & Lindman, 1981). Therefore, the diffusion coefficient reported by the counterion resonances, $D_{\text{obs,Arg}}$, e.g., is given by Eq. 2.

$$D_{\text{obs,Arg}} = f_{\text{b,Arg}}{}^{*} D_{\text{micelle}} + \left(1 - f_{\text{b,Arg}}\right) * D_{\text{free,Arg}} \quad (2)$$

$D_{\text{free,Arg}}$ is the free-solution diffusion coefficient for arginine, $(8.10 \pm 0.02) \times 10^{-10}$ m^2 s^{-1}, and $f_{\text{b,Arg}}$ is the mole fraction of arginine molecules bound to the micelles (Stilbs, 1987). Pulsed-gradient NMR experiments were used to measure $D_{\text{obs,und-Phe}}$, D_{micelle}, $D_{\text{und-Phe,free}}$, $D_{\text{obs,Arg}}$, and $D_{\text{free,Arg}}$. Equations 1 and 2 were then used to calculate $f_{\text{b,und-Phe}}$ and $f_{\text{b,Arg}}$ (or $f_{\text{b,Lys}}/f_{\text{b,ornithine}}$), respectively.

Table 1 reports diffusion coefficients, $f_{\text{b,und-Phe}}$, and R_{h} values for solutions containing 50 mM und-Phe and 50 mM $NaHCO_3$. At 50.0 mM, the surfactant concentration is well above the CMC, so the surfactant molecules exist predominately in micellar form with Na^+ counterions bound to the und-Phe micelle surface. The Table 1 data show that in the pH range 7.5–11.5, the $f_{\text{b,und-Phe}}$ values are all 0.92–0.94 and the micelle radii are 15–16 Å. Therefore, the fraction of surfactant molecules bound to the micelle and the micelle radii remain relatively constant in this pH range.

Previous work showed that und-Leu micelles with Na^+ counterions were somewhat smaller (~11 Å) than the micelles investigated here (Lewis et al., 2016). Furthermore, Ohta, et al. (2006) investigated the phenylalanine-based surfactant, potassium *N*-acyl phenylalaninate. This surfactant contained a 14-carbon hydrocarbon chain containing all C-C single bonds. The und-Phe hydrocarbon chain in contrast contains 11 C atoms, terminated with an alkene. The Ohta et al. study showed that potassium *N*-acyl phenylalaninate aggregated into long nanotubes at approximately 0.2 mM and into micelles at 1.0 mM. However, the micelles formed at higher concentration were approximately 2 nm in diameter and, therefore, much larger than the und-Phe micelles investigated here (Ohta et al., 2006). Micelles formed by lauryl esters of L-phenylalanine

investigated by Vijay et al. (2010a, 2010b) formed large aggregates (50–200 nm) as well. Therefore, comparison with literature results suggests that changes to the length of the hydrocarbon chain and the hybridization of the atoms in the chain cause phenylalanine-based surfactants to form very different aggregates.

Table 1 also reports the hydrodynamic radii of und-Phe micelles with Na^+ counterions measured with DLS. At each pH, there is general agreement between the two techniques. The largest difference in the NMR- and DLS-derived radii (2.3 Å) was measured at pH 9.5. Both the NMR and DLS measurements, however, show that at 50 mM, und-Phe forms relatively small, spherical micelles, and that in the presence of $Na^+_{(aq)}$ counterions, the und-Phe micelles do not become systematically larger or smaller as pH is changed from 7.5 to 11.5.

NMR diffusion experiments were also performed as a function of pH with solutions containing 50 mM und-Phe and 50 mM L-arginine. Diffusion coefficients, $f_{b,Arg}$, $f_{b,und\text{-}Phe}$, and micelle radii from these experiments are shown in Table 2. The fraction of und-Phe molecules bound to the micelles, $f_{b,und\text{-}Phe}$, remained relatively constant over the pH range studied. Table 2 also shows that in the L-arginine-containing solutions, the fraction of L-arginine counterions bound to the micelles, $f_{b,Arg}$, decreased as the pH increased, as did the micelle radii. The change in micelle radii and $f_{b,Arg}$ values with pH are plotted in Fig. 5a. Comparison of radii values in Table 2 with those in Table 1 shows that below pH 9.5, the radii of the micelles in the und-Phe/L-arginine solutions were larger than those in solutions containing und-Phe micelles and Na^+ counterions. This result was likely obtained because the R_h value reports the size of the micelles plus their bound counterions. Arginine molecules are considerably larger than Na^+ cations, so micelles containing L-arginine counterions would be expected to be larger than micelles containing only Na^+.

The decrease in the $f_{b,Arg}$ values and micelle radii with increasing pH will now be addressed. Figure 5a shows that the $f_{b,und\text{-}Phe}$ values remain constant over the pH range studied. This result suggests that the decrease in R_h with pH is not caused by fewer surfactant molecules associating with the micelles at high pH. On the other hand, the pK_a of L-arginine's primary amine functional group is approximately 9.0 (Berg, Tymoczko, Gatto, & Stryer, 2015). Therefore, at this pH, L-arginine molecules begin to change from cationic to zwitterionic form. The decrease in $f_{b,Arg}$ beginning at pH 9.0, therefore, likely results from the L-arginine cations deprotonating and the zwitterionic L-arginine molecules being overall less attracted to the negative micelles. The decrease in $f_{b,Arg}$ is also accompanied by a decrease in R_h. Figure 6a shows a model of L-arginine/und-Phe micelles with the counterions bound perpendicular to the micelle surface. If the L-arginine counterions are bound to the und-Phe micelles in this manner, we would expect that a decrease in R_h would accompany the dissociation of L-arginine from the micelle. Previous work with und-Leu has shown that L-arginine counterions bind perpendicular to the und-Leu micelle surface and dissociate from the und-Leu micelles at high pH in the same manner as proposed here (Lewis et al., 2016). Further evidence for this L-arginine-binding model is provided by the two-dimensional NMR experiments described below.

Table 3 presents diffusion coefficients, fraction bound values, and hydrodynamic radii from experiments with solutions containing 50 mM und-Phe and 50 mM L-lysine. Like the L-arginine studies, the fraction of und-Phe molecules bound to micelles remains relatively constant (0.94–0.95) throughout the pH range. The $f_{b,\ Lys}$ values, though, are approximately 0.4 from pH 7.5–8.5, begin to decrease at pH 9.0, and are only approximately 0.05 at pH 11.5. The change in $f_{b,\ Lys}$ with pH is plotted in Fig. 5b. Therefore, the results in both Table 3 and Fig. 5b suggest that like L-arginine, L-lysine counterions begin to

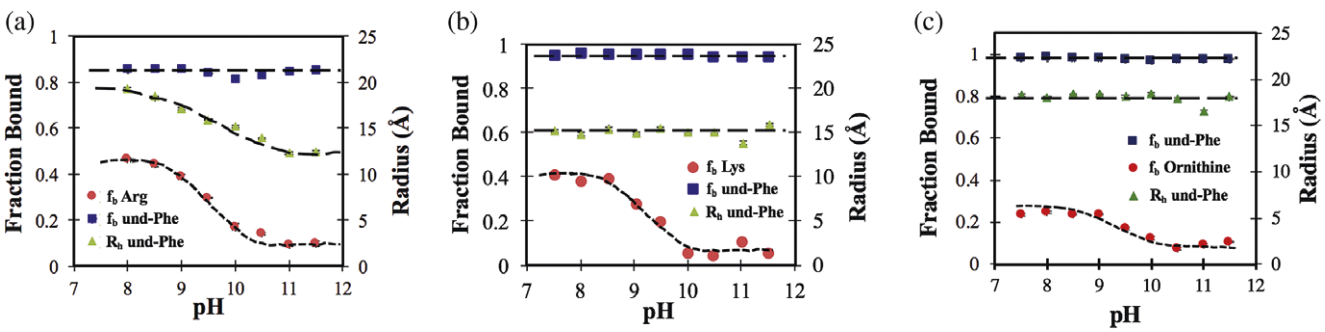

Fig. 5 (**a**) The und-Phe and L-arginine fraction bound values and und-Phe micelle radii *versus* pH for solutions containing 50 mM und-Phe and 50 mM L-arginine; (**b**) und-Phe and L-lysine fraction bound values and und-Phe micelle radii *versus* pH for solutions containing 50 mM und-Phe and 50 mM L-lysine; (**c**) und-Phe and L-ornithine fraction bound values and und-Phe micelle radii *versus* pH for solutions containing 50 mM und-Phe and 50 mM L-ornithine

become zwitterionic around pH 9.0 and then dissociate from the micelle surface (Berg et al., 2015). By pH 11.5, dissociation is nearly complete, with very few L-lysine counterions bound to the micelles.

However, Table 3 also shows that unlike the behavior of the und-Phe/L-arginine micelles, the radii of the und-Phe/L-lysine micelles remains relatively constant (~14–15 Å) throughout the investigated pH range. In other words, when the L-lysine counterions dissociate from the micelle surface beginning at pH 9.0, there is little to no accompanying decrease in micelle size. An analogous result was obtained previously for und-Leu/L-lysine solutions (Lewis et al., 2016). One possible explanation for this result is that L-lysine binds parallel to the und-Phe micelle surface as shown in Fig. 6b, with both its cationic primary and side-chain amines interacting with anionic surfactant monomers. If L-lysine binds to the micelle in this fashion, we would expect relatively little change in the micelle radius when the L-lysine molecules dissociated from the micelle and were replaced with Na^+ ions. This behavior is also shown in Fig. 6b and again is further supported by the two-dimensional NMR experiments described below.

The structures in Fig. 1 show that L-arginine's amino acid side chain contains a three-carbon aliphatic chain bound to a guanidinium functional group. In contrast, L-lysine's side chain contains a four-carbon aliphatic chain bound to a simple amine. Therefore, we might ask the following question. Do L-arginine and L-lysine bind differently to the und-Phe micelles because they contain aliphatic chains of different length or is the difference related to L-arginine and L-lysine containing different functional groups on their amino acid side chains? To address this question, the binding of L-ornithine to the und-Phe micelles was investigated. The structure of L-ornithine is shown in Fig. 1d. This amino acid's side chain contains a three-carbon aliphatic chain (like arginine) bound to an amine functional group (like lysine).

Table 4 and Fig. 5c report diffusion coefficients, f_b values and hydrodynamic radii in the pH range 7.5–11.5 for solutions containing 50.0 mM und-Phe and 50.0 mM L-ornithine. The L-ornithine study showed that the f_b value of the counterion was the highest at pH 7.5, began decreasing at pH 9.0, and was very low at high pH. This behavior is analogous to that observed for L-arginine and L-lysine and is consistent with L-ornithine binding to the und-Phe micelles in cationic form, but dissociating at high pH when the counterions become zwitterionic. In addition, as with L-arginine and L-lysine counterions, in the L-ornithine/und-Phe solution, the $f_{b,\text{und-Phe}}$ values remain relatively high (>0.97) and do not change in the investigated pH range. The und-Phe micelle radii in the L-ornithine-containing solutions also remain relatively constant as a function of pH. This result is analogous to that observed in the L-lysine/und-Phe study and suggests that like L-lysine, L-ornithine binds parallel to the micelle surface as shown in Fig. 6b. Furthermore, the L-ornithine experiments suggest that L-lysine and L-arginine interact differently with the und-Phe micelles because they contain different functional groups on their amino acid side chains and not because their side chains have aliphatic chains of different length. Recall L-ornithine and L-arginine have the same length aliphatic chain, yet the two counterions were found to bind parallel and perpendicular to the micelle surface, respectively.

One notable difference, though, in the binding of L-lysine and L-ornithine to the und-Phe micelles is that at pH values when the binding is strongest, the L-lysine counterion f_b values are significantly larger than those of L-ornithine's. For example, below pH 9.0, the f_b value of L-lysine was approximately 0.40, while the corresponding value for L-ornithine was 0.24. This result suggests that in their cationic forms, L-ornithine has overall less affinity for the und-Phe micelles than L-lysine. It was suggested previously that when L-lysine binds parallel to the micelle surface its two amine functional groups act as a bridge connecting two different surfactant monomers. This behavior is also illustrated in Fig. 4. The shorter amino acid side chain in L-ornithine may make it more difficult for the counterion to bind simultaneously to two surfactant molecules. In other words, in L-ornithine, the two amine functional groups may be too close together to effectively act as a bridge between different surfactant monomers. This effect may in turn decrease L-ornithine's overall micelle-binding affinity compared to that of L-lysine and may lead to the lower counterion f_b values shown in Table 4.

ROESY Analyses

In order to gain further insight into the mechanism of L-arginine and L-lysine association with und-Phe micelles, ROESY spectra were collected for und-Phe/L-arginine and und-Phe/L-lysine mixtures. ROESY is a two-dimensional NMR technique in which cross peaks connect NMR resonances for protons that are within ~5 Å from one another (Bax & Davis, 1985). Intramolecular ROESY cross peaks connect protons within the same molecule, while intermolecular cross peaks connect protons from different molecules that are close together in space. A qualitative approach was used in the work presented here in which the presence, absence, and relative intensities of intermolecular ROESY cross peaks were used to support the L-arginine and L-lysine binding mechanism discussed above (Lewis et al., 2016). An analysis of intramolecular und-Phe cross peaks was performed as well to investigate the orientation of the und-Phe aromatic ring relative to the micelle core. Quantitative ROESY analyses can also be used to measure interatomic

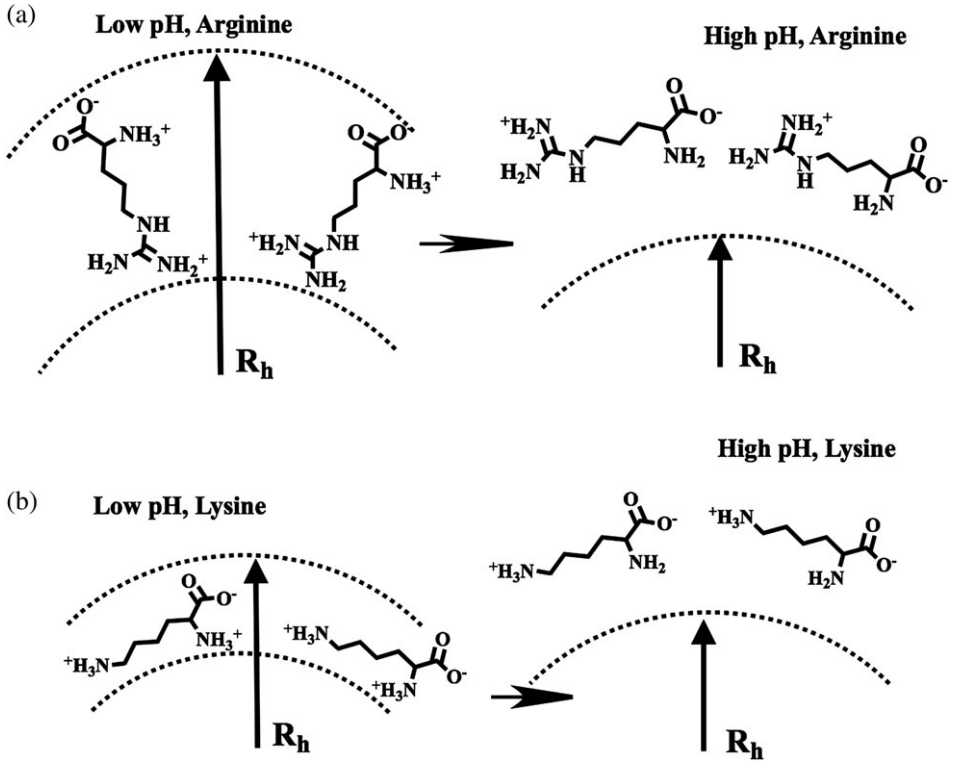

Fig. 6 (**a**) Proposed model of L-arginine binding to and dissociating from und-Phe micelles. Dissociation of L-arginine from the micelle surface is accompanied by a change in the hydrodynamic radius. (**b**) Proposed model of L-lysine binding to and dissociating from und-Phe micelles. Dissociation of L-lysine from the micelle surface is accompanied by little change in the hydrodynamic radius

distances by monitoring ROESY cross peak intensity as a function of mixing time (Ammalahti, Bardet, Molko, & Cadet, 1996; Ganjiwale & Cowsik, 2015; Hilton, Chmurny, & Muschik, 1992; Thiele, Petzold, & Schleucher, 2009). Finally, combining NMR diffusion and two-dimensional NMR experiments has been shown to provide complementary information about the size and structure of micellar aggregates (Cho et al., 2012; Denkova, Van Lokeren, Verbruggen, & Willem, 2008, 2009; Morris, Becker, Valle, Warner, & Larive, 2006).

Figure 7a shows a portion of the ROESY spectrum of a mixture containing 50 mM und-Phe and 50 mM L-arginine at pH 8. In Fig. 7a, the intermolecular cross peaks connecting the L-arginine and und-Phe resonances are assigned and annotated in red. The intermolecular cross peaks observed between the und-Phe aromatic and L-arginine protons are

Table 4 D_{obs} (und-Phe), $D_{micelle}$, $D_{ornithine}$, und-Phe f_b values, L-ornithine f_b values, and micelle hydrodynamic radii (R_h) *versus* pH for und-Phe solutions containing L-ornithine counterions

pH	$D_{obs} \times 10^{10}$ und-Phe ($m^2\ s^{-1}$)	$D_{micelle} \times 10^{10}$ ($m^2\ s^{-1}$)	$D_{ornithine} \times 10^{10}$ ($m^2\ s^{-1}$)	f_b und-Phe	f_b L-ornithine	R_h (Å) (NMR)
7.5	1.40 (±0.01)	1.32 (±0.01)	7.24 (±0.02)	0.982 (±0.017)	0.236 (±0.004)	18.3 (±0.1)
8.0	1.41 (±0.01)	1.33 (±0.01)	7.15 (±0.01)	0.983 (±0.017)	0.248 (±0.004)	18.1 (±0.1)
8.5	1.41 (±0.01)	1.31 (±0.01)	7.23 (±0.01)	0.979 (±0.017)	0.237 (±0.004)	18.4 (±0.1)
9.0	1.45 (±0.01)	1.33 (±0.01)	7.42 (±0.01)	0.974 (±0.017)	0.213 (±0.004)	18.1 (±0.1)
9.5	1.44 (±0.01)	1.31 (±0.01)	7.75 (±0.04)	0.972 (±0.016)	0.169 (±0.006)	18.4 (±0.1)
10.0	1.49 (±0.01)	1.35 (±0.01)	8.11 (±0.06)	0.969 (±0.017)	0.124 (±0.009)	17.9 (±0.2)
10.5	1.57 (±0.01)	1.46 (±0.01)	8.51 (±0.02)	0.976 (±0.017)	0.073 (±0.005)	16.5 (±0.1)
11.0	1.44 (±0.01)	1.32 (±0.01)	8.37 (±0.04)	0.974 (±0.017)	0.090 (±0.006)	18.3 (±0.1)
11.5	1.44 (±0.01)	1.33 (±0.01)	8.25 (±0.02)	0.976 (±0.017)	0.106 (±0.004)	18.1 (±0.1)

At each pH, the und-Phe concentration was 50.0 mM and the temperature was 25.0°C.

also listed in Table 5. All other resonances shown in the Fig. 7a spectrum are intramolecular cross peaks connecting the und-Phe aromatic and und-Phe NH resonances to other surfactant peaks. The presence of intermolecular cross peaks between the und-Phe and L-arginine resonances show that their corresponding protons are within ~5 Å from one another and confirms that L-arginine cations are bound to the und-Phe micelles at pH 8. In addition, Fig. 7a and Table 5 show that the cross peaks between the und-Phe aromatic and Arg-H_δ resonances are much stronger than the corresponding cross peaks between und-Phe aromatic and Arg-H_α resonances. In fact, no und-Phe to Arg-H_α cross peaks are visible at the contour level chosen in the Fig. 7a spectrum. In addition, Table 4 also shows that relatively weak cross peaks were observed between the und-Phe and the Arg-H_γ and Arg-H_β protons as well. This result suggests that the Arg-H_δ protons are on average closer to the und-Phe micelle surface and that the Arg-H_α, H_β, and H_γ protons are farther away.

Figure 7b shows one-dimensional projected spectra obtained from the ROESY spectrum in Fig. 7a. Projections were made parallel to the F1 axis along each of the data points defining, respectively, the Arg-H_δ, H_γ, H_β, and H_α resonances in the F2 dimension. These one-dimensional spectra contain peaks from all the protons that showed a ROESY cross peak with each of the respective L-arginine protons. In these projected spectra, each peak's area is proportional to the distance between the corresponding L-arginine proton and the resonance shown in the spectrum (Morris et al., 2006). The spectra in Fig. 7b are expanded to show only the und-Phe aromatic protons and the und-Phe H_β resonance.

The projected spectra in Fig. 7b show that L-arginine H_δ is on average closer than H_α, H_β, and H_γ to the und-Phe protons and the micelle surface, as evidenced by the much more intense peaks observed for the L-arginine H_δ trace in Fig. 7b. This finding suggests that arginine counterions bind to the und-Phe micelles perpendicular to the micelle surface and primarily through the cationic guanidinium functional group on the amino acid side-chain. Note that the guanidinium functional group is connected to the carbon atom containing the L-arginine H_δ protons. In the bound state, the rest of the arginine molecule extends into free solution and away from the micelle surface. In this arrangement, the arginine H_α, H_β, and H_γ protons are farther from the und-Phe protons, thus leading to the weaker cross peaks observed in the ROESY spectra. Overall, it can be concluded that both the NMR diffusion and ROESY results point to the same model of und-Phe micelle/L-arginine counterion association.

A ROESY spectrum was also collected for a mixture containing und-Phe micelles and L-lysine counterions at pH 8. The intermolecular cross peaks observed in this spectrum are given in Table 5. Figure 7c shows projections taken along the lysine H_α, H_β, H_δ and H_ε resonances in this ROESY spectrum using the method described above. The spectra are again expanded to show only und-Phe aromatic peaks. As in Fig. 7b, the area of the peaks in Fig. 7c is proportional to the distance between the und-Phe aromatic and L-lysine protons (Xing et al., 2008). A trace for lysine H_γ is not shown because its resonance and an und-Phe peak overlapped. The Fig. 7c spectra suggest that all of the L-lysine protons are a comparable distance from the und-Phe protons (and thus the micelle surface) because the peaks in each trace of Fig. 7c have a comparable intensity or area. Therefore, the L-lysine ROESY results are consistent with the diffusion results, in that both analyses suggest that unlike L-arginine, L-lysine binds parallel to the und-Phe micelle surface with both its primary and side chain amine functional groups interacting with anionic surfactant monomers.

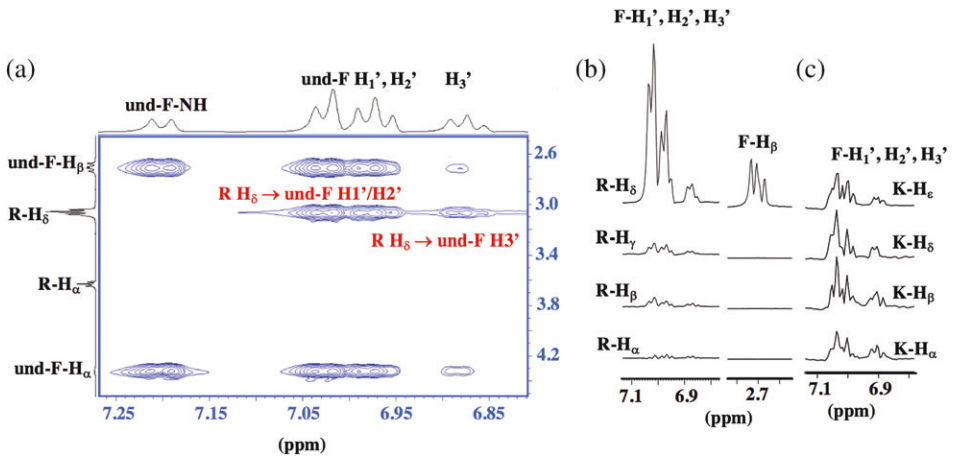

Fig. 7 (**a**) ROESY spectrum of 50 mM und-Phe (F) and 50 mM L-arginine (R) at pH 8. Red assignments indicate an intermolecular cross peak. (**b**) One-dimensional projections from the ROESY spectrum in (**a**). (**c**) One-dimensional projections from a ROESY spectrum of 50 mM und-Phe and 50 mM L-lysine (K) at pH 8.0

Table 5 Summary of intermolecular cross peaks from ROESY spectra of mixtures containing 50 mM und-Phe either 50 mM L-arginine or 50 mM L-lysine at pH 8.0

L-Arginine protons (ppm)	ROESY cross peak to und-Phe (ppm)		
H_α (3.63)		Not observed	
H_β (1.76)	H_1',H_2' weak (7.00)	H_3' weak (6.88)	
	NH weak (7.20)		
H_γ (1.54)	H1′,H2′ weak (7.00)	H3′ weak (6.88)	
	NH weak (7.20)		
H_δ (3.06)	H_α (4.33)	H_β (2.71)	H_1 (1.92)
	H_1', H_2' (7.01)	H_3' weak (6.88)	
L-Lysine protons (ppm)	ROESY cross peak to und-Phe (ppm)		
H_α (3.63)	H_1', H_2' (7.040)	H_3' (6.903)	
H_β (1.778)	H_1', H_2' (7.040)	H_3' (6.903)	NH (7.196)
H_δ (1.58)	H_1', H_2' (7.040)		
H_ε (2.89)	(H_1', H_2') (7.040)	H_3' (6.903)	

Table 6 Summaries of intramolecular cross peaks from ROESY spectra of 50 mM und-Phe and either 50 mM L-arginine or 50 mM L-lysine at pH 8

und-Phe aromatic protons (ppm) (arginine)	ROESY cross peak to und-Phe (ppm)		
H_1', H_2' (7.0264)	H_α (4.316)	H_1 (1.908)	H_3–H_7 (1.106)
	H_β (2.711)	H_2 (1.248)	H_8 (0.749)
H_3' (6.8828)	H_α (4.316)	H_1 (1.908)	H_3–H_7 (1.106)
	H_β (2.711)	H_2 (1.248)	H_8 (0.749)
und-Phe aromatic protons (lysine)	ROESY cross peak to und-Phe (ppm)		
H_1', H_2' (7.040)	H_α (4.334)	H_2 (1.116)	H_8 (0.742)
	H_β (2.700)	H_3–H_7 (0.967)	H_1 (1.908)
H_3' (6.903)	H_α weak (4.334)	H_2 (1.116)	H_8 (0.742)
	H_β weak (2.700)	H_3–H_7 (0.967)	H_1 (1.908)

Finally, in a study by Vijay et al. (2010a, 2010b), NMR spectroscopy was used to study amphiphilic laurel esters of L-phenylalanine. This cationic surfactant contained a dodecyl hydrocarbon tail connected to L-phenylalanine by an ester bond. When this surfactant formed micelles, the phenylalanine aromatic ring was found to be rotated toward the micelle's hydrocarbon core (Vijay et al., 2010a, 2010b). ROESY results presented below indicate that the aromatic ring of und-Phe behaves similarly by also rotating toward the core of the und-Phe micelles.

Figure 8 shows a portion of the ROESY spectrum of a mixture containing 50 mM und-Phe and 50 mM L-arginine. This ROESY spectrum shows a number of intramolecular cross peaks connecting the und-Phe aromatic ring peaks to other und-Phe resonances. In Fig. 8, a green box is drawn around these cross peaks. All of these cross peaks connecting the und-Phe aromatic resonances to other und-Phe protons are reported in Table 6 for spectra collected with 50 mM und-Phe and 50 mM L-arginine, and 50 mM und-Phe and 50 mM L-lysine. Table 6 and Fig. 8 show ROESY cross peaks between the phenylalanine aromatic resonances (H_1', H_2', and H_3') and und-Phe protons H_1, H_2, $H_{3–7}$, and H_8 on the surfactant's hydrocarbon chain. See Fig. 1 for

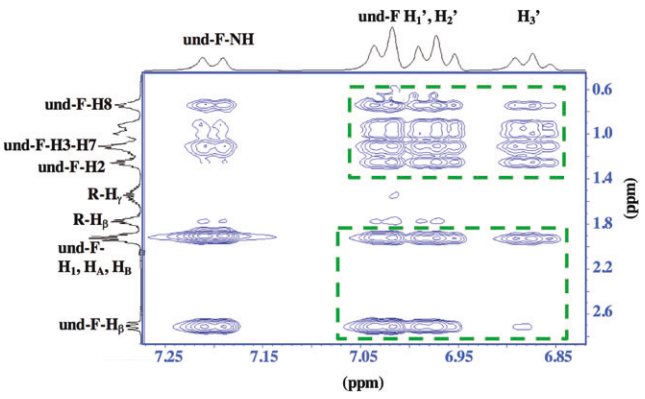

Fig. 8 A portion of the ROESY spectrum of a 50 mM und-Phe and 50 mM L-arginine solution at pH 8. The green boxes identify cross peaks connecting the und-Phe aromatic resonances to other und-Phe protons

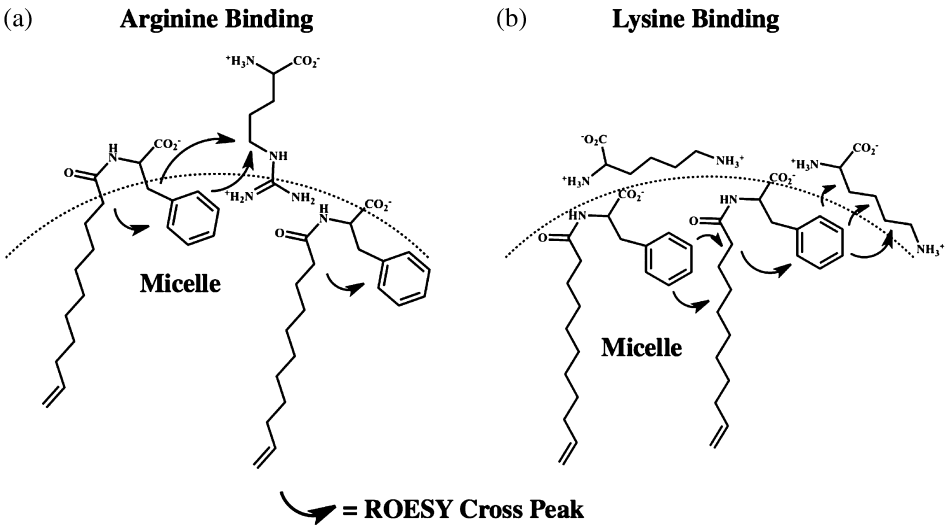

Fig. 9 Models of (**a**) und-Phe/L-arginine and (**b**) und-Phe/lysine micellar complexes. The arrows indicate cross peaks observed in the ROESY spectra. Cationic forms of the amino acid counterions found in solution below pH 9.0 are shown

proton labels. Similar ROESY cross peaks were also detected in the study by Vijay et al. (2010a,2010b). Therefore, the Table 6 and Fig. 8 results strongly suggest that in the und-Phe/L-arginine micelle solutions, the aromatic ring of the surfactant rotates toward the micelle core, thus placing the protons on the aromatic ring close to the hydrocarbon chain protons. Table 6 also lists cross peaks observed in a ROESY spectrum of a mixture containing 50 mM und-Phe and 50 mM L-lysine. The cross peaks in this spectrum were nearly identical to those observed in und-Phe/L-arginine mixture. Therefore, in the und-Phe/L-lysine micelle solutions, the und-Phe aromatic ring is also likely rotated toward the micelle hydrocarbon core.

Conclusions

Micelle formation by the amino acid-based surfactant und-Phe was investigated from pH 7.5 to 11.5. The surfactant had a lower CMC at low pH and a higher CMC in more basic solutions. At low pH, surfactant solutions containing L-arginine and L-lysine counterions had lower CMC values than solutions containing Na^+ counterions. This result was consistent with a study of fatty acid aggregation by Koyama, which found that bulky counterions like L-arginine lead to lower fatty acid CMC values (Koyama, 2005). Both NMR and DLS experiments showed that und-Phe surfactants with Na^+ counterions formed relatively small micelles with hydrodynamic radii of approximately 15 Å. Micelle radii also did not change appreciably with pH when Na^+ counterions were present. In solutions containing L-arginine, L-lysine, and L-ornithine counterions, the mole fraction of micelle-bound counterions was the highest at a low pH when the amino acids were cationic, but much lower at high pH when the counterions converted to zwitterionic form. When L-arginine counterions dissociated from the micelle at high pH, the micelle hydrodynamic radii also decreased. In contrast, micelle radii remained relatively constant as a function of pH in the presence of L-lysine and L-ornithine counterions. Two-dimensional ROESY experiments were used to further investigate the structure of the und-Phe/counterion complexes. A model consistent with the two-dimensional NMR and counterion binding studies is shown in Fig. 9 with arrows depicting cross peaks observed in the ROESY spectra. Figure 9 shows L-arginine counterions attaching perpendicular to the micelle surface through the guanidinium functional group on the amino acid's side chain. On the other hand, L-lysine is shown to bind parallel to the und-Phe micelle surface with both its primary and side chain amines interacting with anionic surfactant molecules. Finally, ROESY experiments also suggested that in the und-Phe micelles, the aromatic rings on the und-Phe phenylalanine headgroup rotated toward the hydrocarbon core. This orientation is also depicted in Fig. 9.

Acknowledgements This work was supported by an NSF-RUI grant (no. 1213532) to Drs. F. H. B. and K. F. M., a Robert A. Welch Chemistry Departmental Grant to the Chemistry Program at Texas A&M University-Corpus Christi, an NSF CAREER grant (no. 0449742) to Dr. E. J. B., a Howard University Medicine Alumni Association Endowed Founder's Chair in Basic Science award and an Office of Naval Research (no. N00014-17-1-2105) grant to Dr. Y. F., and an NIH-NIMHD grant (no. G12 MD007579) to the RCMI Program at Howard University. We also acknowledge the generosity of the Ralph E. Klingenmeyer family and thank Professor John Kirk for his help with the DLS measurements.

References

Ammalahti, E., Bardet, M., Molko, D., & Cadet, J. (1996) Evaluation of distances from ROESY experiments with the intensity-ratio method. *Journal of Magnetic Resonance Series A*, **122**:230–232.

Annunziata, O., Costantino, L., D'Errico, G., Paduano, L., & Vitagliano, V. (1999) Transport properties for aqueous sodium sulfonate surfactants: 2. Intradiffusion measurements: Influence of the obstruction effect on the monomer and micelle Mobilities. *Journal of Colloid and Interface Science*, **216**:16–24.

Bax, A., & Davis, D. G. (1985) Practical aspects of two-dimensional transverse NOE spectroscopy. *Journal of Magnetic Resonance*, **63**: 207–213.

Begotka, B. A., Hunsader, J. L., Oparaeche, C., Vincent, J. K., & Morris, K. F. (2006) A pulsed field gradient NMR diffusion investigation of enkephalin peptide-sodium dodecyl sulfate micelle association. *Magnetic Resonance in Chemistry*, **44**:586–593.

Berg, J. M., Tymoczko, J. L., Gatto Jr., G. J., & Stryer, L. (2015) *Biochemistry* (8th ed.). New York: WH Freeman and Company.

Bijma, K., & Engberts, J. B. F. N. (1997) Effect of counterions on properties of micelles formed by alkylpyridinium surfactants. 1. Conductometry and ^{1}H-NMR chemical shifts. *Langmuir*, **13**: 4843–4849.

Bordes, R., & Holmberg, K. (2015) Amino acid-based surfactants – Do they deserve more attention? *Advances in Colloid and Interface Science*, **222**:79–91.

Brito, R. O., & Silva, S. (2011) Enhanced interfacial properties of novel amino acid-derived surfactants: Effects of headgroup chemistry and of alkyl chain length and unsaturation. *Colloid Surface B*, **86**:65–70.

Chandra, N., & Tyagi, V. K. (2013) Synthesis, properties, and applications of amino acids based surfactants: A review. *Journal of Dispersion Science and Technology*, **34**:800–808.

Cho, C., Mao, J., Li, F., Yang, M., He, H., Jiang, L., & Liu, M. (2012) Understanding the interaction between valsartan and detergents by NMR techniques and molecular dynamics simulation. *The Journal of Physical Chemistry B*, **116**:7470–7478.

Clapes, P., & Infante, M. (2002) Amino acid-based surfactants: Enzymatic synthesis, properties and potential applications. *Biocatalysis and Biotransformation*, **20**:215–233.

Covington, C. L., & Polavarapu, P. L. (2016) Concentration dependent specific rotations of chiral surfactants: Experimental and computational studies. *The Journal of Physical Chemistry. B*, **120**: 5715–5725.

Denkova, P. S., Van Lokeren, L., Verbruggen, I., & Willem, R. (2008) Self-aggregation and supramolecular structure investigations of Triton X-100 and SDP2S by NOESY and diffusion ordered NMR spectroscopy. *The Journal of Physical Chemistry B*, **112**: 10935–10941.

Denkova, P. S., Van Lokeren, L., Verbruggen, I., & Willem, R. (2009) Mixed micelles of Triton X-100, sodium dodecyl dioxyethylene sulfate, and Synperonic L61 investigated by NOESY and diffusion ordered NMR spectroscopy. *The Journal of Physical Chemistry B*, **113**:6703–6709.

D'Errico, G., Ornella, O., Paduano, L., & Vitagliano, V. (2001) Transport properties of aqueous solutions of alkyltrimethylammonium bromide surfactants at 25 degrees C. *Journal of Colloid and Interface Science*, **239**:264–271.

Fournial, A. G., Zhu, Y., Molinier, V., Vermeersch, G., Aubry, J. M., & Azaroual, N. (2007) Aqueous phase behavior of tetraethylene glycol decanoyl ester (C9COE4) and ether (C10E4) investigated by nuclear magnetic resonance spectroscopic techniques. *Langmuir*, **23**:11443–11450.

Ganjiwale, A., & Cowsik, S. M. (2015) Membrane-induced structure of novel human tachykinin hemokinin-1 (hHK1). *Biopolymers*, **103**:702–710.

Gnezdilov, O. L., Zuev, Y. F., Zueva, O. S., Potarikina, K. S., & Us'yarov, O. G. (2011) Self-diffusion of ionic surfactants and counterions in premicellar and micellar solutions of sodium, lithium, and cesium dodecyl sulfates as studied by NMR diffusometry. *Applied Magnetic Resonance*, **40**:91–103.

Hilton, B. D., Chmurny, G. N., & Muschik, G. M. (1992) Taxol: Quantitative internuclear proton-proton distances in $CDCl_3$ solution from nOe data: 2D nmrROESY buildup rates at 500 MHz. *Journal of Natural Products*, **55**:1157–1161.

Infante, M., Perez, L., Pinazo, A., & Vinardell, M. P. (2004) Amino acid-based surfactants. *Green Chemistry*, **7**:583–592.

Joondan, N., Jhaumeer-Laulloo, S., & Caumul, P. (2014) A study of antibacterial activity of L-phenylalanine and L-tyrosine esters in relation to their CMCs and their interactions with 1,2-dipalmitoyl-sn-glycero-3-phosphocholine, DPPC a model membrane. *Microbiological Research*, **169**:675–685.

Koyama, M. (2005) Effect of arginine as a counterion on surfactant properties of fatty acid salts. *Journal of Dispersion Science and Technology*, **26**:785–789.

Lewis, C., Hughes, B. H., Vasquez, M., Wall, A. M., Northrup, V. L., Witzleb, T. J., … Morris, K. F. (2016) Effect of pH on the binding of sodium, lysine, and arginine counterions to L-undecyl leucinate micelles. *Journal of Surfactants and Detergents*, **19**:1175–1188.

Lipidot, Y., Rappoport, S., & Wolman, Y. J. (1967) Use of esters of *N*-hydroxysuccinimide in the synthesis of *N*-acylamino acids. *Journal of Lipid Research*, **8**:142–145.

MacInnis, J. A., Palepu, R., & Marangoro, D. G. (1999) A nuclear magnetic resonance investigation of the micellar properties of a series of sodium cyclohexylalkanoates. *Canadian Journal of Chemistry*, **77**:1994–2000.

Morris, K. F., Becker, B. A., Valle, B. C., Warner, I. M., & Larive, C. K. (2006) Use of NMR binding interaction mapping techniques to examine interactions of chiral molecules with molecular micelles. *The Journal of Physical Chemistry B*, **110**: 17359–17369.

Morris, K. F., Gao, X., & Wong, T. C. (2004) The interactions of the HIV gp41 fusion peptides with zwitterionic membrane mimics determined by NMR spectroscopy. *Biochimica et Biophysica Acta (BBA): Biomembranes*, **1667**:67–81.

Ohta, A., Danev, R., Nagayama, K., Mita, T., Asakawa, T., & Miyagishi, S. (2006) Transition from nanotubes to micelles with increasing concentration in dilute aqueous solution of potassium N-acyl phenylalaninate. *Langmuir*, **22**:8472–8477.

Orfi, L., Lin, M., & Larive, C. K. (1998) Measurement of SDS micelle-peptide association using ^{1}H NMR chemical shift analysis and pulsed-field gradient NMR spectroscopy. *Analytical Chemistry*, **70**:1339–1345.

Phani Kumar, B. V. N., Priyadharsini, S. U., Prameela, G. K. S., & Mandal, A. B. (2011) NMR investigations of self-aggregation characteristics of SDS in a model assembled tri-block copolymer solution. *Journal of Colloid and Interface Science*, **360**:154–162.

Piotto, M., Saudek, V., & Skienar, V. (1992) Gradient-tailored excitation for single quantum NMR spectroscopy of aqueous solutions. *Journal of Biomolecular NMR*, **2**:661–665.

Ramos, Z., Rothbauer, G., Turner, J., Lewis, C., Morris, K. F., Billiot, E. J., … Fang, Y. (2017) Comparison of chiral recognition of binaphthyl derivatives with L-undecyl-leucine surfactants in the presence of arginine and sodium counterions. *Journal of Chromatographic Science*. Manuscript submitted for publication.

Sciba, G. (2016) Chiral recognition in separation science-an update. *Journal of Chromatography A*, **1467**:56–78.

Shimizu, S., Pires, P. A. R., & El Seoud, O. A. (2003) ^{1}H and ^{13}C NMR study on the aggregation of (2-acylaminoethyl) trimethylammonium chloride surfactants in D_2O. *Langmuir*, **19**:9645–9652.

Singh, G., Singh, G., & Kang, T. S. (2016) Micellization behavior of surface active ionic liquids having aromatic counterions in aqueous media. *The Journal of Physical Chemistry B*, **120**:1092–1105.

Sreenu, M., Prasad, R. B. N., Sujitha, P., & Kumar, C. G. (2015) Synthesis and surface-active properties of sodium N-acylphenylalanines and their cytotoxicity. *Industrial and Engineering Chemistry Research*, **54**:2090–2098.

Stilbs, P. (1987) Fourier transform pulsed gradient spin echo studies of molecular diffusion. *Progress in Nuclear Magnetic Resonance Spectroscopy*, **19**:1–45.

Stilbs, P., & Lindman, B. (1981) Determination of organic counterion binding to micelles through Fourier transform NMR self-diffusion measurements. *The Journal of Physical Chemistry*, **85**:2587–2589.

Thiele, C. M., Petzold, K., & Schleucher, J. (2009) EASY ROESY: Reliable cross-peak integration in adiabatic symmetrized ROESY. *Chemistry A European Journal*, **15**:585–588.

Varka, E. M., Coutouli-Argyropoulou, E., Infante, M. R., & Pegiadou, S. (2004) Synthesis, characterization, and surface properties of phenylalanine-glycerol ether surfactants. *Journal of Surfactants and Detergents*, **7**:409–414.

Vijay, R., Baskar, G., Mandal, A. B., & Polavarapu, P. L. (2013) Unprecedented relationship between the size of spherical chiral micellar aggregates and their specific optical rotations. *The Journal of Physical Chemistry. B*, **117**:3791–3797.

Vijay, R., Mandal, A. B., & Baskar, G. (2010a) Amphilic lauryl ester derivatives from aromatic amino acids: Significance of chemical architecture in aqueous properties. *The Journal of Physical Chemistry. B*, **114**:13959–13970.

Vijay, R., Mandal, A. B., & Baskar, G. (2010b) ^{1}H NMR spectroscopic investigations on the conformation of amphiphilic aromatic amino acid derivatives in solution: Effect of chemical architecture of Amphiphiles and polarity of solvent medium. *The Journal of Physical Chemistry B*, **114**:13691–13702.

Vitiello, G., Ciccarelli, D., Ortona, O., & D'Errico, G. (2009) Microstructural characterization of lysophosphatidylcholine micellar aggregates: The structural basis for their use as biomembrane mimics. *Journal of Colloid and Interface Science*, **336**:827–833.

Wu, D., Chen, A., & Johnson Jr., C. S. (1995) An improved diffusion ordered spectroscopy experiment incorporating bipolar gradient pulses. *Journal of Magnetic Resonance*, **115**:260–264.

Xing, H., Lin, S. S., Lu, R. C., & Xian, J. X. (2008) NMR investigation on micellization of ammonium/tetraalkylammonium perfluorooctanoates. *Colloids and Surfaces A: Physicochemical and Engineering Aspects*, **318**:199–205.

Biographies

Gabriel Rothbauer was an undergraduate research student at Carthage College before graduating in 2017. His research used NMR spectroscopy and dynamic light scattering to study amino acid-based surfactants.

Elisabeth Rutter was an undergraduate research student at Carthage College before graduating in 2017. At Carthage she used NMR spectroscopy to characterize amino acid-based surfactants.

Chelsea Reuter-Seng was an undergraduate research student at Carthage College before graduating in 2016. Her research at Carthage used NMR spectroscopy to characterize amino acid-based surfactants.

Simon Vera is an undergraduate research student at Texas A&M Corpus Christi. His research uses NMR and fluorescence spectroscopy to measure critical micelle concentrations and aggregation numbers of amino acid-based surfactants.

Eugene Billiot is a professor of chemistry at Texas A&M Corpus Christi. His research investigates the factors responsible for chiral recognition with media designed for use as chiral pseudostationary phases in capillary electrophoresis.

Yayin Fang is an associate professor in the Department of Biochemistry and Molecular Biology at Howard University. Her research uses computer modeling to investigate interactions between low molecular weight compounds and targets such as polymers, nucleic acids and proteins.

Fereshteh Billiot is an associate professor of chemistry at Texas A&M Corpus Christi. Her work involves the synthesis and characterization of amino acid-based surfactants, their characterization with fluorescence spectroscopy, and their use as chiral selectors in capillary electrophoresis.

Kevin Morris is a professor of chemistry at Carthage College. His research uses NMR spectroscopy and molecular dynamics simulations to investigate the structure and dynamics of chiral surfactant micelles.